Contributions of a Strengthened Early Holocene Monsoon and Sediment Loading to Present-Day Subsidence of the Ganges-Brahmaputra Delta

Mikhail Karpytchev, V. Ballu, Y. Krien, Melanie Becker, S. Goodbred, G. Spada, S. Calmant, C. K Shum, Z. Khan

Contributions of a strengthened early Holocene monsoon and sediment loading to present-day subsidence of the Ganges-Brahmaputra Delta

M. Karpytchev[1], V. Ballu[1], Y. Krien[1], M. Becker[1], S. Goodbred[2], G. Spada[3], S. Calmant[4], C.K. Shum[5, 6] and Z. Khan[7]

[1] LIENSs UMR 7266 CNRS, University of La Rochelle, La Rochelle, France

[2]Department of Earth and Environmental Sciences, Vanderbilt University, Nashville, Tennessee, USA

[3]Dipartimento di Scienze Pure e Applicate (DISPeA), University of Urbino "Carlo Bo", Urbino, Italy

[4]LEGOS UMR5566/CNRS/CNES/IRD/UPS, France

[5]School of Earth Sciences, Ohio State University, Columbus, Ohio, USA

[6]Institute of Geodesy and Geophysics, Chinese Academy of Sciences, Wuhan, China

[7]Institute of Water Modelling, Dhaka, Bangladesh

Corresponding author: mikhail.karpytchev@univ-lr.fr

This article has been accepted for publication and undergone full peer review but has not been through the copyediting, typesetting, pagination and proofreading process which may lead to differences between this version and the Version of Record. Please cite this article as doi: 10.1002/2017GL076388

Abstract

The contribution of subsidence to relative sea-level rise in the Ganges-Brahmaputra delta (GBD) is largely unknown and may considerably enhance exposure of the Bengal basin populations to sea level rise and storm surges. This paper focuses on estimating the present-day subsidence induced by Holocene sediment in the Bengal basin and by oceanic loading due to eustatic sea level rise over the past 18 kyr. Using a viscoelastic Earth model and sediment deposition history based on in-situ measurements, results suggest that massive sediment influx initiated in the early Holocene under a strengthened South Asian monsoon may have contributed significantly to the present-day subsidence of the GBD. We estimate that the Holocene loading generates up to 1.6 mm/yr of the present-day subsidence along the GBD coast, depending on the rheological model of the Earth. This rate is close to the 20th century global mean sea level rise (1.1-1.7 mm/yr). Thus, past climate change, by way of enhanced sedimentation, is impacting vulnerability of the GBD populations.

Keywords: Ganges-Brahmaputra delta; land subsidence; sediment loading; relative sea level change;

Key Points :

- Holocene sediment/ocean loads generate up to 1.6 mm/yr of the present-day subsidence in the Ganges-Brahmaputra delta
- Highest subsidence rates occur at the Bengal coast and the subaqueous delta
- Past climate affects present-day vulnerability of the Bengal basin populations

1. Introduction

The densely populated Ganges-Brahmaputra delta (GBD) is among the most exposed low-lying regions (Fig.1) of the world where the future sea level rise has the potential to induce large land loss and put millions of people at risk [Nicholls, 2011; IPCC AR5, 2013]. Like in the majority of large deltas [Syvitski et al., 2009], subsidence contributes to relative sea level rise along the GBD coast and results in faster rates than those driven solely by climate-induced global sea level [Ostanciaux et al., 2012; Pethick and Orford, 2013; Brammer, 2014; Woppelmann and Marcos, 2016]. In the GBD, the trends in coastal tide gauge records are typically about 4-6 mm/yr [Brown and Nichols, 2015]. By this way, the GBD subsidence increases the exposure of the Bengal basin populations to flooding and erosion [Ericson et al., 2006] and the practical need for a regional climate adaptation strategy calls for measuring, understanding and predicting the delta subsidence as a contributor to rates of local sea level rise.

The limited studies to date suggest great variability in the rates of subsidence throughout the GBD, although these results are determined by methods that consider a variety of spatial and temporal scales. Using Interferometric Synthetic Aperture Radar (InSAR) and GNSS (Global Navigation Satellite System) techniques, Higgins et al. [2014] and Steckler et al. [2012] detected present-day subsidence rates varying between 0 and 18 mm/yr in different areas of the GBD. The expected spatial and temporal variability of land subsidence rates results from interaction of numerous natural processes that may also be enhanced by human activities [Syvitski et al., 2009]. These natural processes include Earth deformation induced by sediment/water loading, sediment compaction and tectonic movements as the Bengal basin is situated in an area of strong deformation and faulting related to the subduction/collision of the Indian plate with the Burma arc [Alam et al., 2003; Steckler et al., 2008, 2016].

A particular feature of the GBD is that sediment supply, dispersion and deposition are mainly driven by runoff from the South Asian monsoon [Goodbred, 2003]. Present-day annual average of the cumulative runoff in the GBD is about 1100 mm/yr [Milliman and Farnsworth, 2013] (ranking it among the five largest world rivers) and, following the monsoon, the runoff experiences large seasonal variations. The enormous mass of water discharged by the rivers during the summer monsoon induces more than 5 cm of seasonal elastic flexure of the GBD [Steckler et al., 2010, Chanard et al., 2014]. While this seasonal water loading and unloading induce mostly elastic response of the Earth, continuously

deposited sediments generate a significant viscous deformation of the Earth's mantle [Haskell, 1935]. The climate changes regulating the monsoons strength are thus imprinted in the variability of sediment loading on the Bengal basin. Currently, the GBD transports about ~1.1 Gt/yr (1Gt = 10^9t) of sediments corresponding to annually average sediment yield of about 500 t/km^2/yr [Milliman and Syvitski, 1992]. The huge amount of sediment drained by the GBD places it, together with Huanghe (Yellow) and the Amazon river, among the three world largest sediment-carrying rivers [Milliman and Farnsworth, 2013]. The sediments were stored over the past 7 kyr, in approximately equal parts, on the subaerial delta, subaqueous delta and canyon-fan system of the Bay of Bengal. During the Early Holocene, ca. 11 – 7 kyr B.P., the sediment discharge was greater by a factor of 2.3, at least, due to the strengthened South Asian monsoon at that time and an abundance of stored hillslope and valley sediment in the Himalaya [Goodbred and Kuehl, 2000a; Goodbred, 2003]. The purpose of this paper is to quantify the contribution of the Holocene sediment/water loading to the present-day land subsidence in the GBD region. To address these issues we model the Earth's deformation, for a range of plausible lithosphere-mantle structures, induced by (1) the recent and Holocene deposition of sediments in the Bengal basin and on the deep-sea Bengal fan and (2) water loading due to eustatic sea level rise in the Bay of Bengal since 18 kyr B.P.

2. Model

We consider the Earth as a Maxwell viscoelastic, spherically symmetric, self-gravitating, incompressible planet with density and elastic parameters of the Preliminary Reference Earth Model PREM [Dziewonski and Anderson, 1981]. The Earth's deformation is computed by the TABOO software [Spada, 2003] that has been extensively used and benchmarked in post-glacial rebound modeling [Spada et al., 2011]. TABOO was designed for solving equations of linear viscoelasticity in a spherically symmetric planet with a given number of layers of different viscosity and elastic parameters.

2.1. Loading history

The surface loads are represented in the model by a set of spherical disks of angular radius 0.25° (≈28 km) [James and Ivins, 1998]. The thickness of each disk varies according to history of sediment storage and sea level changes at a given site. It is difficult to construct an ocean loading model specific to the Bay of Bengal as there are no published curves of Holocene relative sea changes for this region. We employed the eustatic sea level curve of Lambeck et al. [2014] to construct a model of ocean loading in the Bay of Bengal over the

past 18 kyr. Milne and Mitrovica (2008) demonstrated large regional deviations of sea level from the globally averaged eustatic value. Particularly in the Bay of Bengal, the sea level was predicted to stand by about 15 m below the eustatic value at 21 kyr B.P. and by 5 m at 6 kyr B.P. [Milne and Mitrovica, 2008]. Thus, the regional sea level departures should have increased the subsidence in the Bay of Bengal but in seeking for minimum subsidence estimate we do not take this effect into account (Supplementary Material provides some estimates of the impact of regional departures in the Holocene sea level on the subsidence of the Bay of Bengal).

History of sediment deposition in the model is displayed in Fig. 2a. The higher sedimentation rates on the upper fan at 15 kyr B.P. correspond to growing sediment discharge and precipitation after the arid period in the South Asia climate [Duplessy et al., 1982; Gasse et al., 1991; Kudrass et al., 2001]. During 15-11 kyr B.P., most of the Bengal basin remained exposed and the lowstand river valleys were connected to the Swatch of No Ground canyon system, leading to sediments largely bypassing the delta and the shelf and being exported to the Bengal fan [Kuehl et al., 2005]. We assume that variations in thickness of sediments accumulated on the upper fan are similar to variations in radiocarbon-dated sequences measured in situ by Weber et al. [1997] in sediment cores. At about 11.9 kyr B.P. corresponding, in the model, to the end of the Younger Dryas, the sediment storage on the upper fan is set to the current rate of 0.3 Gt/yr (Fig.2a). At that time, rapidly increasing Holocene sea level and flooding of the Bengal basin trapped river sediment in the GBD, sustaining rapid long-term sedimentation rates of 1 cm/yr or more [Goodbred and Kuehl, 1999, 2000b]. Sediment deposition across the upper fan is supposed to be spatially uniform at the scale of thousands of years as suggested by high-resolution multichannel seismic surveys [France-Lanord et al., 2000; Schwenk et al., 2003]. We thus neglect a thickening of sediment cover in the channel-levee system of the Swatch of No Ground canyon [Hübscher and Spieβ, 2005] and thinning of the Holocene sediment layer at the continental slope [Contreras-Rosales et al., 2014], because in terms of loading impact, these features represent localized mass anomalies that barely affect delta subsidence [Wolstencroft et al., 2014]. A total thickness of 10 m of sediment accumulated on the upper fan is used in the model which is in agreement with the observed Holocene cores heights [Weber et al., 1997; Hein et al., 2017]. This value is likely an overestimate of the spatially averaged thickness of the Holocene sediment on the upper fan [Contreras-Rosales et al., 2014] but the lack of data does not allow constraining it with more accuracy. Nevertheless, as the recent analysis by Palemenghi et al.

[2011] suggests a smaller portion of sediment transported to the fan than used in this study, we have run the model also with much slower sediment accumulation rates on the upper fan (section 4S in Supplementary Material) in order to evaluate the impact of the upper fan sediment loading on the GBD vertical movement.

On the subaqueous delta and flood plain of the Bengal basin, the history of sedimentation was constructed from the isopach map (Fig.2b) and sediment storage rates (Fig.2a) established by Goodbred and Kuehl [2000a] from borehole data (see Supplementary Material for more details). Rate of sediment accumulation on the flood plain in the Early Holocene, over 11-7 kyr B.P., is set to 2.3 Gt/yr. From 7 kyr B.P up to present it equals 0.35 Gt/yr [Goodbred and Kuehl, 2000a]. The subaqueous delta begins to form in the model at 7 kyr B.P. (Fig.2a) with a constant sediment deposition rate of 0.35 Gt/yr [Kuehl et al. 1997]. Time-histories of sediment storage on the flood plain and subaqueous delta (Fig.2a) were rescaled before setting them as disks' thicknesses to ensure that (1) the present-day net sediment thickness of every disk corresponds to that on the observation-based isopach map by Goodbred and Kuehl [2000a] and (2) the net volume of sediments stored within the Bengal Basin is partitioned as evaluated by Goodbred and Kuehl [2000a], namely: 5×10^{12} m^3 of sediments being sequestered during the 11-7 kyr B.P period and 3.5×10^{12} m^3 since then. In order to convert sediment volume to mass, we followed Goodbred and Kuehl [2000a] and used bulk density values of 1.5×10^3 kg/m^3 and 1.8×10^3 kg/m^3 for the post-7 kyr and older sediments, respectively, in agreement with Japan International Cooperation Agency [1976], Weber et al. [2005] and Brammer [2012]. On the flooded or submarine disks, when deposited sediments displace water, we use the difference in density between sediments and water to compute additional load.

2.2 The lithosphere and mantle structure

There are a lot of uncertainties on lithosphere-mantle structure and viscosity beneath the Bengal Basin [Alam et al., 2003] . Confined between the stable Indian craton in the west and the tectonically active Burma thrust fold belt in the east, the GBD is flanked by the Indian Ocean in the south and the Himalayas in the north. This tectonically complex environment probably generates strong lateral rheology contrasts underneath the Bengal Basin that cannot

be constrained without using much more subsidence data along with seismic and gravity observations [Gasperini, et al., 1990; Karpychev and Fleitout, 2000; Spada et al., 2006; Whitehouse, et al., 2006; Steffen et al., 2007]. The lateral viscosity variations may induce variations in subsidence rates for different regions in the GBD. However, Krien et al. [2016] showed that the order of magnitude of subsidence rates and the first-order basin scale deformation pattern in the GBD are correctly captured by laterally uniform models. Structural and mineralogical heterogeneities in the lower continental crust and the upper mantle can also result in much more complex deformation of the Bengal basin than that described by a single-viscosity Maxwell rheology model [Ivins and Sammis, 1996; Han et al. 2006; Caron et al., 2017]. However the lack of observational constraints on the Holocene deformation rates in the GBD does not allow distinguishing between complex viscosity structures. To estimate the plausible response of the GBD to the Holocene sediment and ocean loading we explore a set of laterally uniform lithosphere-mantle structures derived mostly from Glacial Isostatic Adjustment (GIA) models.

Below we present the results for three depth-dependent mantle viscosities corresponding to a hard, intermediate and soft mantle with different lithospheric thicknesses. First, we consider a hard sub-cratonic structure by a 90-km thick lithosphere underlain by an upper mantle with viscosity of 0.5×10^{21} Pa×s and a lower mantle with viscosity of 2×10^{21} Pa×s (Fig.2c). This viscosity model is close to models VM2 and VM5a [Peltier, 2004; Peltier and Drummond, 2008] which explain well the relative sea level histories in Fennoscandia [Peltier, 2004, Argus and Peltier, 2010], North America [Paulson et al., 2007] and the sea level response to sediment loading in the Indus River along the western side of the Indian craton [Ferrier et al., 2015]. (Computations for a 90-km thick lithosphere and a more viscous mantle are presented in Supplementary Material). Our intermediate model is composed of a thinner 50-km thick lithosphere, a softer upper mantle with viscosity of 1×10^{20} Pa×s and a lower mantle viscosity of 2×10^{21} Pa×s, the same as in the hard rheology Earth described above. The parameters of the intermediate model are in the 95%-confidence limits of the optimal global values assessed by Lambeck et al. [2014]. The Bengal Basin is considered as a remnant ocean basin [Ingersoll et al., 1995; Alam et al., 2003] squeezed between the Indian and Burma plates [Steckler et al., 2008]. By analyzing seismic receiver functions Mitra et al. [2005] detected the presence of oceanic crust in the North of the Bengal basin. Mall et al. [1999], also based on seismic observations, pointed to a rather weak mantle beneath the Bengal basin that they interpreted as a trace of a mantle plume originated in the Indian Ocean and having crossed the mantle below the Bengal basin before producing the Rajmahal Traps (Fig.1) [Curray and Munasinghe, 1991; Muller et al., 1993]. In view of these considerations we tested a weak structure with a 40-km thick lithosphere underlain by an asthenosphere extending to the depth of 220 km. The viscosity of the asthenosphere is set to 3×10^{19} Pa×s and that of the underlying shallow upper mantle is 3×10^{20} Pa×s. Viscosity of the upper mantle below the 400 km depth is 5×10^{20} Pa×s and that of the lower mantle equals 2×10^{21} Pa×s. It is worth noting that the

viscosity profiles described above were chosen to cover a range of plausible responses of the Earth to the Holocene sediment/ocean loading of the Bengal basin. None of these lithosphere-mantle structures should be preferred unless observations can validate the model. **3. Predicted Subsidence**

The sediment and ocean loading sequences applied over the past 18 kyr generate a basin-wide subsidence of the GBD (Fig.3) for all rheological structures presented above. Maximum rates are located on the subaqueous delta between Sundarbans and the submarine canyon "Swatch of No Ground". Interestingly, Kuehl et al. [1989] and Michels et al. [2003] measured the highest current sediment accumulation rates (up to 5-20 cm/yr) in this part of the Bengal shelf. We suggest that the enhanced subsidence in this area contributed, on thousand-year time scale, to the intensified sedimentation in the upper reaches of the canyon [Kuehl et al., 2005]. We propose that the location of maximum subsidence between the GBD coast and the subaqueous delta is due to partitioning of sediment/ocean load between the GBD flood plain, subaqueous delta and the fan of the Bay of Bengal. As expected, a thicker lithosphere results in a more widespread deformation and smaller amplitude of subsidence rates. The Earth strength at shallow depths controls the amplitude of the subsidence [Ivins et al., 2007]. A weaker structure composed of thinner lithosphere and/or less viscous mantle enhances maximum of the present-day subsidence (Fig.3). For this reason, the highest rate of subsidence is obtained in the weak lithosphere-mantle model (Fig.3c): It reaches ~ 1.6 mm/yr versus 1.1 mm/yr for the hard rheology model (Fig.3a). It is worth noting that sediment loading in our model is based on minimum estimates of sediment deposited in the Bengal Basin, as sediment cores in the lower delta plain extend only to 90 m and did not reach the lowstand surface or sediment deposits older than ~12 kyr [Goodbred and Kuehl, 2000a]. Consequently, the modeled subsidence rates represent a minimum subsidence driven by Holocene sedimentation. As expected from Peltier [2004], we observed that the present-day subsidence rates are not very sensitive to magnitude of the lower mantle viscosity. This is due to relatively small horizontal dimensions of the Bengal basin (300-500 km) so that increasing the lower mantle viscosity by a factor of 10 modifies the Earth's surface subsidence by ~ 0.1 mm/yr.

The net subsidence predicted by our model (Fig.4) shows how much the Pleistocene-Holocene boundary has subsided over the past 18 kyr, with one of mantle-lithosphere structures displayed in Fig.2c. The model with the weakest Earth structure (Fig.4c) provides the largest subsidence. With this model, the Bengal coast and the subaqueous delta were lowered by about 30-35 m since 18 kyr B.P. This implies that a large fraction of

accommodation for delta progradation was created by the Earth viscoelastic response to the GBD sediment/water loading [Watts, 2001; p. 150-165]. Notice also an impact of loading on steepening of the initial delta slope [Hutton et al., 2013] which is produced by the model with all lithosphere-mantle structures: The coast and subaqueous delta in Fig.4 subsided by about 20-35 m vs. 5-10 m of net subsidence in the northern Bengal Basin. Fig.5 displays time-varying subsidence curves and subsidence rates at several selected sites. The magnitude of subsidence differs from one site to another, but with all rheological structures, roughly half of load-induced accommodation space at each site was created during the period of the strengthened monsoon, between 11 and 7 kyr B.P. The remaining half of subsidence occurred during the late delta development from 7 kyr B.P. to present.

It is of interest that before the flood plain sedimentation started at 11 kyr. B.P., the weak mantle model predicts an uplift at all sites (Fig.5). This uplift corresponds to a landward bulge generated by initial loading of the GBD by upper fan sediments and the eustatic sea level rise. Its amplitude varies spatially and is more than 1 m at Hatiya, Chittagong and Dhaka. The impact of this landward bulge on the delta development can be twofold as it reduces accommodation space but increases steeping of the delta slope [Watts, 2001, p.150-165]. The fastest land subsidence in the GBD was generated by enhanced sedimentation on the flood plain between 11 and 7 kyr B.P (Fig.5) At that time, subsidence rates were about 3-5 times larger than the present-day value depending on the site location and the rheological model of the Earth. In the current vertical land movement, the effect of the early Holocene monsoon has waned to a considerable extent but is still present. As demonstrated in Fig.5, the subsidence rates will change little in forthcoming hundreds of years due to the relatively slow Earth viscoelastic relaxation

The model results should be compared with the subsidence measured over thousand-year time period [Wolstencroft et al., 2014] but these observations are scarce and depend on the eustatic sea level reconstruction in the Bay of Bengal. Brown and Nicholls [2015] have estimated a median of reported Holocene subsidence rates to be 2 mm/yr with a standard deviation of about 5 mm/yr. There is, seemingly, a general agreement [Akter et al., 2015] that the Holocene subsidence rates are about 1-5 mm/yr on the flood plain with a tendency to increase towards the GBD margin [Umitsu, 1993; Stanley and Hait, 2000; Goodbred and Kuehl, 2000b; Allison and Kepple, 2001; Sincavage et al., 2017]. The subsidence rates predicted by our model are in the range of rates derived from these observations.

On the shelf, Hübscher and Spieβ [2005] have pointed to an apparent contradiction between the assumed subsidence rates of 2-4 mm/yr and the lowstand paleoshoreline depth of 120-130 m measured by [Wiedicke et al., 1999] at 21°N / 90°E about 100 km south of the GBD coast. Such subsidence rate would have resulted, over a 20 kyr period, in a net subsidence of the Bengal shelf of 40-80 m. However, the present-day paleoshore depth is comparable with the estimated eustatic sea level stand at the time of Last Glacial Minimum (LGM) between -135 m and -130 m, suggesting a net shelf subsidence of only a few meters [Lambeck et al, 2014]. In the present study, our model predicts a net subsidence at the shoreline of Wiedicke et al. [1999] of 22 (Fig.4a) to 32 m (Fig.4c) when the thick lithosphere-hard mantle is replaced by a weaker rheological structure. This 20-30 m net subsidence indicates, perhaps, a regional departure of the Holocene sea level in the Bay of Bengal from the global average that is typical for the rapid sea level rise during the major phase of deglaciation over 16.5-7 kyr B.P. [Milne and Mitrovica, 2008; Lambeck et al., 2014]. Finally, our model does not account for late glacial unloading of the GBD margin due to erosion that might have led to uplift of the shelf prior to the Holocene flooding and sedimentation and explains the present-day depth of the paleoshore.

4. Conclusions

We used published Holocene sediment storage history of Goodbred and Kuehl [2000a] and the eustatic sea level curve of Lambeck et al. [2014] to estimate present-day and cumulative loading-induced subsidence of the Bengal Bay and the GBD. Calculated rates differ depending on the values used for lithospheric thickness and viscosity of the upper mantle. Spatially, maximum subsidence occurs along the central GBD coast and adjacent subaqueous delta, where calculated subsidence rates vary from 1.1 mm/yr considering a cratonic-like mantle to 1.6 mm/yr using a thin lithosphere and weak upper mantle. Thus the impact of Holocene sedimentation is far from negligible, as it causes the Bengal coast to subside at a rate comparable to the global average rate of sea level rise during the last century (1.1-1.7 mm/yr) [Church and White, 2011; Hay et al, 2015]. Subsidence rates have also varied through time, as riverine sediment supply and delta accumulation have varied with intensity of the South Asia monsoon and the rate of sea level rise. Maximum rates occurred in the early Holocene, coincident with peak fluvial sediment discharge and rapid glacio-eustasy.

This contribution of Holocene sedimentation to subsidence of the Bengal delta is inescapable in the sense that this subsidence will continue for the next hundreds/thousands years because

of the Earth's "viscous memory", even if the sedimentation is stopped. However, Holocene sedimentation is not the only driver of GBD subsidence. Recent measures of present-day subsidence yield local rates up to 10-20 mm/yr in some areas [Steckler et al., 2012; Higgins et al., 2014] notably in the densely populated city of Dhaka. Holocene sediment/water loading contributes relatively little to these hot spots of land subsidence in the GBD which are mostly due to groundwater extraction and sediment compaction [Higgins et al., 2014] similarly to other deltas [Teatini et al., 2011; Erban et al., 2014; Brain, 2016]. It is on the larger spatial scale where the sediment loading contribution to the GBD movement becomes pronounced. Often, the effects of sediment loading are not taken into account but this background contribution should not be neglected for closing the total subsidence budget in the deltas. The isolation and accurate partitioning of subsidence due to non-loading drivers induced by natural or anthropogenic processes which is needed for prediction of future subsidence [Jones et al., 2016] and elaboration of climate adaptation strategies must account for the large scale signal due to sediment/ocean loading.

Acknowledgements

We are grateful to Hermann Kudrass, Torbjörn Törnqvist, anonymous Reviewer and the Editor, M. Bayani Cardenas, for the constructive insights and suggestions that helped to improve this study. We acknowledge funding support from the Belmont Forum/IGFA G8, the BanD-AID project, http://Belmont-BanDAiD.org, via ANR in France, NSF in the US, and DFG in Germany. GS was supported by a DisPeA research grant. The source code and data for TABOO software used in this study are freely available from one of the authors (GS) or from https:// github.com/danielemelini/TABOO.

References

Akter, J., Sarker, M.H., Popescu, I., and Roelvink, D. (2015) Evolution of the Bengal Delta and its prevailing processes, J. Coastal Res., 32(5), 1212-1226, doi: 10.2112/JCOASTRES-D-14-00232.1

Alam, M., M. M. Alam, J. R. Curray, M. L. R. Chowdhury and M.R. Gani (2003) An overview of the sedimentary geology of the Bengal basin in relation to the regional tectonic framework and basin-fill history, *Sediment. Geol.*, 155, 179–208, doi:10.1016/S0037-0738(02)00180-X

Allison, M., and Kepple, E. (2001) Modern sediment supply to the lower delta plain of the Ganges-Brahmaputra River in Bangladesh: *Geo-Marine Letters*, v. 21, p. 66–74, doi:10.1007/s003670100069

Argus, D.F. and W.R. Peltier (2010) Constraining models of postglacial rebound using space geodesy: a detailed assessment of model ICE-5G(VM2) and its relatives, *Geophys. J. Int*,181, 697-723, doi: 10.1111/j.1365-246X.2010.04562.x

The Antarctica component of postglacial rebound model ICE-6G_C (VM5a) based on GPS positioning, exposure dating of ice thicknesses, and relative sea level histories, *Geophys. J. Int*, 198, 537-563.

Brammer, H. (2012) The physical geography of the soils of Bangladesh. *University Press Ltd.*, Dhaka.

Brammer, H. (2014) Bangladesh's dynamic coastal regions and sea-levl rise, *Climate Risk Management*, 1, 51-62

Brain, M.J., (2016) Past, Present and future perspectives of sediment compaction as a driver of relative sea level and coastal change, *Curr. Clim. Change Rep., 2*, 75–85, doi:10.1007/s40641-016-0038-6

Brown, S. and R. J. Nicholls (2015) Subsidence and human influences in mega deltas: The case of the Ganges-Brahmaputra-Meghna, *Science Total Envir.*, 527-528, 362-374.Caron, L. et al., (2017), Inverting glacial isostatic adjustment signal using Bayesian framework and two linearly relaxing rheologies, *Geophys. J. Int., 209*, 1126—1147

Chanard, K., Avouac, J.P., Ramillien G., and J. Genrich (2014) Modeling deformation induced by seasonal variations of continental water in the Himalaya region: Sensitivity to Earth elastic structure, J. Geophys. Res., 119, 5097–5113, doi:10.1002/2013JB010451

Church, J. and N. White (2011) Sea level rise from the late 19th to the early 21st century, *Surv. Geophys.* 32, 585-602, doi:10.1007/s10712-011-9119-1

Contreras-Rosales, L.A., T. Jennerjahn, T., Tharammal, T., V. Meyer, A. Luckge, A. Paul, E. Schefuβ (2014) Evolution of the Indian Summer Monsoon and terrestrial vegetation in the Bengal region during the past 18 ka, *Quaternary Sci. Rev.*, 102, 133-148, http://dx.doi.org/10.1016/j.quascirev.2014.08.010

Curray, J. R. and T. Munasinghe (1991) Origin of the Rajmahal Traps and the 85◦E Ridge: Preliminary reconstructions of the trace of the Crozet hotspot; *Geology* 19, 1237-1240

Dziewonski, A.M. and Anderson, D.L.(1981) Preliminary reference Earth model. *Phys. Earth Planet. Inter.*, 25: 297-356

Duplessy, J.C. (1982) Glacial to interglacial contrasts in the northern Indian Ocean. *Nature,* v.295, pp. 494-498Erban, L.E, S.M. Gorelick and H.A. Zebker (2014) Ground water extraction, land susbidence and sea-level rise in the Mekong Delta, Vietnam, *Environ. Res. Lett.*,9, doi:10.1088/1748-9326/9/8/084010

Ericson, J.P., C.J. Vörösmarty, S.L. Dingman, L.G. Ward and M. Meybeck (2006) Effective sea-level rise and deltas: causes of change and human dimension implications, *Global Planet Change* 50, 63-82

Ferrier, K. L., J. X. Mitrovica, L. Giosan and P. D. Clift (2015) Sea-level responses to erosion and deposition of sediment in the Indus River basin and the Arabian Sea. *Earth Planet. Sci. Lett.*, 416, 12-20

France-Lanord, C., V. Spiess, P. Molnar and J. Curray (2000) Summary on the Bengal Fan. An Introduction to a Drilling Proposal. *Woods Hole Oceanographic Institution*.

Gasse, F., M. Arnold, J.C. Fontes, M. Fort, E. Gilbert, A. Huc, L. Bingyan, L. Yuanfan, L. Qing, F. Mélières,E. Van Campo,W. Fubao and Z. Quingsong (1991) A 13,000-year climate record from western Tibet: Nature, v. 353, p. 742–745

Gasperini, P., D.A. Yuen and R. Sabadini (1990) Effects of lateral viscosity variations onpost-glacial rebound: implications for recent sea-level trends, Geophys. Res. Lett., 17(1),5-8

Goodbred, S.L. and S.A. Kuehl (1999) Holocene and modern sediment budgets for the Ganges-Brahmaputra river system: Evidence for highstand dispersal to fllod-plain, shelf, and deep-sea depocenters, *Geology*, 27(6), 559-562

Goodbred, S.L. and S.A. Kuehl (2000a) Enormous Ganges-Brahmaputra sediment discharge during strengthening early Holocene monsoon, *Geology*, 28(12),1083-1086

Goodbred, S.L. and S.A. Kuehl (2000b) The significance of large sediment supply, active tectonism, and eustasy on margin sequence development: Late Quaternary stratigraphy and evolution of the Ganges-Brahmaputra Delta, *Sediment. Geol.*, 133, 227–248, doi:10.1016/ S0037-0738(00)00041-5

Goodbred, S. (2003) Response of the Ganges dispersal system to climate change: a source-to-ling view since the last interstade, *Sedim. Geology*, 162, 83-104

Han, S.-K., C.K. Shum, M. Bevis, C. Ji, and C.Y. Kuo (2006) Crustal dilatation observed by GARCE after the 2004 Sumatra-Andaman earthquake, *Science*, 313, 658—662

Haskell, N.A., 1935, The motion of a viscous fluid under a surface load: Journal of Applied Physics, v. 6, p. 265–269, doi:10.1063/1.1745329

Hay, C.C, E. Morrow, E., R.E. Kopp and J. Mitrovica (2015) Probabilistic reanalysis of twentieth-century sea-level rise, *Nature*, doi:10.1038/nature14093

Hein, C.J., V. Galy, A. Galy, C. France-Lanord, H. Kudrass, and T. Schwenk (2017) Post-glacial climate forcing of surface processes in the Ganges-Brahmaputra river basin and implications for carbon sequestration, *Earth Planet. Sci. Lett.*, 478, 89-101

Higgins, S.A., I. Overeem, M.S. Steckler, J.P.M. Syvitski, L. Seeber and S.H. Akhter (2014) InSAR measurements of compaction and subsidence in the Ganges-Brahmaputra Delta, Bangladesh, *J. Geophys. Res.*, 119, 1768-1781, doi:10.1002/2014JF003117.

Hübscher, C. and Spieβ, V. (2005) Forced regression systems tracts on the Bengal Shelf, *Marine Geology*, 219, p. 207-218

Hutton, E.W.H., J.P.M. Syvitski, A.B. Watts (2013) Isostatic flexure of a finite slope due to sea-level rise and fall, *Computers & Geosciences*, 53, 58-68

Ingersoll, R.N., Graham, S.A., Dickinson, W.R., 1995 Remnant ocean basins in Busby, C.J., Ingersoll, R.V. (Eds.), *Tectonics of Sedimentary Basins*, Blackwell, 363-391

IPCC AR5 Climate Change 2013: The Physical Science Basis. Working Group I Contribution to the Fifth Assessment Report of the Intergovernmental Panel on Climate Change (Stocker TF, et al., eds.). Cambridge, United Kingdom and New York, NY:Cambridge University Press (2014)

Ivins, E.R., C.G. Sammis (1996) Transient creep of a composite lower crust 1.Constitutive theory, J. Geophys. Res., 191, B12, 27981-28004

Ivins, E.R., R.K Dokka and R.G. Blom (2007) Post-glacial sediment load and subsidence in coastal Louisiana, *Geophys. Res. Lett.*, 34, L16303, doi:10.1029/2007GL030003

Ivins, E.R. , C.A. Raymond and T.S. James (2000) The influence of 5000 year-old and younger glacial mass variability on present-day crustal rebound in the Antarctic Peninsula, *Earth, Planets and Space, 52*, 1023-2019

James, T.S. and E.R. Ivins (1998) Predictions of Antarctic crustal motions driven by present-day ice sheet evolution and by isostatic memory of the Last Glacial Maximum, *J. Geophys. Res.*, 103(B3), 4993-5017

Japan International Cooperation Agency, 1976, Geology and stone material: Jamuna Bridge Construction Project: Tokyo, *Japan International Cooperation Agency*, 54 pp.

Jones, C.E., K. An, R.G. Blom, J.D. Kent, E.R Ivins, and D. Bekaert (2016) Anthropogenic and geologic influences on subsidence in the vicinity of New Orleans, Louisiana, J. Geophys. Res. Solid Earth, 121, 3867-3887, doi:10.1002/2 015JB012636

Karpychev, M. and L. Fleitout (2000), Long-wavelength geoid : the effect of continental roots and lithosphere thickness variations, *Geophys. J. Int.*, v. 143(3), pp. 945-963.

Krien, Y., C. Mayet, L. Testut, F. Durand, A.R. Tazkia , A.K.M.S. Islam, V.V. Gopalakrishna, M. Becker, S. Calmant, C.K. Shum, Z.K. Khan, F. Papa, V. Ballu (2016) Improved bathymetric dataset and tidal model for the head Bay of Bengal, *Marine Geodesy*, 39, 422-438

Krien, Y., M. Karpytchev, V. Ballu, S. Calmant, C.K. Shum. Subsidence due to Holocene sediment load in the Ganges-Brahmaputra delta. *AGU Fall Meeting*, Poster 2016

Kuehl, S.A., T.M. Hariu, and W.S. Moore (1989) Shelf sedimentation off the Ganges-Brahmaputra River system: Evidence for sediment bypassing to the Bengal fan, *Geology*, 17, 1132-1135

Kuehl, S.A., B. M. Levy, W. S. Moore and M. A. Allison (1997) Subaqueous delta of the Ganges-Brahmaputra river system, *Marine Geology*, 144, 81-96

Kuehl, S.A., M.A. Allison, S. L. Goodbred and H. Kudrass (2005) The Ganges-Brahmaputra delta, in *River Deltas- Concepts, Models, and Examples*, SEPM Special Publ. No. 83, ISBN 1-56576-113-8, p. 413–434

Kudrass, H.R., A. Hofmann, H. Doose, K. Emeis and H. Erlenkeuser (2001) Modulation and amplification of climatic changes in the Northern Hemisphere by the Indian summer monsson during the past 80 k.y., *Geology*, 29(1), 63-66

Lambeck, K., H. Rouby, A. Purcell, Y. Sunc, and M. Sambridge (2014) Sea level and global ice volumes from the Last Glacial Maximum to the Holocene, *PNAS*, v.111, n.43

Mall D.M., V.K. Rao and P.R. Reddy (1999) Deep sub-crustal features in the Bengal basin: seismic signatures for plume activity, *Geophys. Res. Lett.*, v. 26, pp. 2545 - 2548

Michels, K.H., A. Suckow, M., Breitzke, H.-R. Kudrass, and B. Kottke (2003) Sediment transport in the shelf canyon “Swatch of No Ground" (Bay of Bengal): *Deep-Sea Reserch II*, 50, 1003-1022

Milliman, J.D., and J.P.M. Syvitski, (1992) Geomorphic/tectonic control of sediment discharge to the ocean: The importance of small mountainous rivers: *J. Geology* 100, 525-544

Milliman, J.D. , K.L. Farnsworth (2013) River discharge to the coastal ocean. A global synthesis, 384 pp., Cambridge Univ. Press

Milne, G.A. and J.X. Mitrovica (2008) Searching for eustasy in deglacial sea-level history, *Quaternary Sci. Rev.*, 27, 2292-2302, doi:10.1016/j.quascirev.2008.08.018

Mitra, S., K. Priestley, A. Kr. Bhattacharyya, and V. K. Gaur (2005), Crustal structure and earthquake focal depths beneath northeastern India and southern Tibet, *Geophys. J. Int.*, 160, 227–248, doi:10.1111/j.1365-246 X.2004.02470.x

Muller R D, Royer J-Y, and Lawver L A 1993 Revised plate motion relative to the hotspots from combined with Atlantic and Indian Ocean hotspot tracks; *Geology* 21, 275-278

Nicholls, R.J. (2011) Planning for the impacts of sea level rise. *Oceanography* 24(2):144–157, doi:10.5670/oceanog.2011.34

Ostanciaux, E., Husson, L., Choblet, G., Robin, C. and Pedoja, K. (2012) Present-day trends of vertical ground motion along the coast lines, *Earth-Science Reviews* 110, 74–92

Palamenghi, L., T. Schwenk, V. Spiess, H. Kudrass (2011) Seismostratigraphic analysis with centennial to decadal time resolution of the sediment sink in the Ganges-Brahmaputra subaqueous delta, *Continental Shelf Res.*, 31, 712-730

Paulson, A., S. Zhong and J. Whar (2007) Inference of mantle viscosity from GRACE and relative sea level data, *Geophys. J. Int.*, 171, 497-508

Peltier, W. R. (2004), Global glacial isostasy and the surface of the ice-age Earth: The ICE-5G (VM2) model and GRACE, *Annu Rev Earth Planet Sci*, *32*, 111–149.

Peltier, W. R., and R. Drummond (2008) The rheological stratification of the lithosphere: A direct inference based upon the geodetically observed pattern of the glacial isostatic adjustment of the North American continent, *Geophys. Res. Lett.*, 35, L16314, doi:10.1029/ 2008GL034586

Pethick, J. and Orford, J.D. (2013) Rapid rise in effective sea-level in southwest Bangladesh: its cause and contemporary rates, *Global Planet Change*, 111, 237-245

Pickering, J.L.,S.L. Goodbred, M. Reitz, T.R. Hartzog, D.R. Mondal, and Md.S. Hossain, (2014) Holocene channel avulsions inferred from the Late Quaternary sedimentary record of the Jamuna and Old Brahmaputra river valleys in the upper Bengal delta plain. *Geomorphology*, 227: 123-136

Pickering, J.L.,S.L. Goodbred, J.C. Beam, J.C. Ayers, A. Covery, H.M. Rajapara, A.K. Singhvi (2017) Terrace development in the upper Bengal basin since the middle Pleistocene: History of Brahmaputra-Jamuna delta construction during multiple highstands, *Basin Research*, 1–18, doi: 10.1111/bre.12236.

Reitz, M.D., J.L. Pickering, S.L. Goodbred, C. Paola, M. Steckler, and L. Seeber (2015) Effects of tectonic deformation and sea level on river path selection: theory and application to Bangladesh. *J. Geophys. Res. – Earth Surface*, 120 (4), 671-689.

Sincavage, R., Goodbred, S., Pickering, J. (2017) Holocene Brahmaputra River path selection and variable sediment bypass as indicators of fluctuating hydrologic and climate conditions in Sylhet Basin, Bangladesh. *Basin Research*, 1-19. doi: 10.1111/bre.12254

Schwenk, T., V. Spieβ, C. Hubscher, M. Breitzke (2003) Frequent channel avulsions within the active channel-levee system of the middle Bengal Fan—an excep-tional channel–levee development derived from Parasound and Hydrosweep data. *Deep-Sea Res. II*, Top. Stud. Oceanogr.50, 1023–1045

Spada, G.(2003) The Theory behind TABOO, *Samizdat Press, Golden, Colorado, 108 pp*

Spada, G., A. Antonioli, S. Cianetti and C. Giunchi (2006) Glacial isostatic adjustment and relative sea level changes: the role of lithospheric and upper mantle heterogeneities in a 3-D spherical Earth,

Geophys. J. Int., 165, 692-702

Spada, G., V.R. Barletta, V. Klemann, R.E.M. Riva, Z. Martinec, P. Gasperini, B. Lund, D. Wolf, L.L.A. Vermeersen and M.A. King (2011) A benchmark study ffor glacial isostatic adjustment codes, *Geophys. J. Int.*, 185, 106-132

Stanley, D.J. and A.K. Hait (2000) Holocene Depositional Patterns, Neotectonics and Sundarban Mangroves in the Western Ganges-Brahmaputra Delta, *J. Coastal Res.*, 16, 26-39

Steckler, M.S., S. H. Akhter, and L. Seeber (2008) Collision of the Ganges-Brahmaputra Delta with the Burma Arc: Implications for earthquake hazard, *Earth Planet. Sci. Lett.*, 273, 367–378, doi:10.1016/j.epsl.2008.07.009

Steckler, M.S., S.L. Nooner, S.H. Akhter, S.K. Chowdhure, S. Bettadpur, L. Seeber and M.G. Kogan (2010) Modeling Earth deformation from monsoonal flooding in Bangladesh using hydrographic, GPS, and Gravity Recovery and Climate Experiment (GRACE) data., *J. Geophys. Res.*, 115, B08407, doi:10.1029/2009JB007018

Steckler, M. et al., (2012) GPS Velocities and Structure Across the Burma Accretionary Prism and Shillong Anticline in Bangladesh, *AGU Fall Meeting Abstracts ， 2012AGUFM.T51F2667S*

Stecker, M.S., D. R. Mondal, S.H. Akhter, L. Seeber, L. Feng, J. Gale, E.M. Hill, and M. Howe (2016) Locked and loading megathrust linked to active subduction beneath the Indo-Burman Ranges, *Nature Geosciences*, 9, 615-618, doi:10.1038/ngeo2760

Steffen, H., P. Wu and G. Kauffmann (2007) Sensitivity of crustal veloctities in Fennoscandia to radial and lateral viscosity variations in the mantle, *Earth Planet. Sci. Lett.*, 257, 474–485, doi: 10.1016/j.epsl.2007.03.002

Syvitski, J.P., A. Kettner, I. Overeem, E.W.H. Hutton, M.T. Hannon, G.R. Brakenridge, J. Day, C. Vorosmarty, Y. Saito, L. Giosan and R.J. Nicholls (2009) Sinking deltas due to human activites, *Nature Geosciences*, doi:10.1038/NGEO0629

Teatini P., L. Tosi , T. Strozzi (2011) Quantitative evidence that compaction of Holocene sediments drives the present land subsidence of the Po Delta in Italy. *J. Geophys. Res.Solid Earth*, 116, B08407, doi:10.1029/2010JB008122

Umitsu, M. (1993) Late Quaternary sedimentary environments and landforms in the Ganges delta: *Sedimentary Geology*, v. 83, p. 177–186

Watts, A. B. (2001) Isostasy and Flexure of the Lithosphere, *Cambridge Univ. Press*

Weber, M.E., M.H. Wiedicke, H.R. Kudrass, C. Hubscher, and H. Erlenkeuser (1997) Active growth of the Bengal fan during sea-level rise and highstand, *Geology*, 25, 315-318

Weber, M.E., M. Wiedicke-Hombach, H.R. Kudrass, H. Erlenkeuser (2005) Bengal Fan sediment tansport activity and response to climate frocing inferred from sediment physical properties, *Sedimentary Geology*, 155, 361-381

Whitehouse, P., K. Latychev, G. A. Milne, J. X. Mitrovica, and R. Kendall (2006), Impact of 3-D Earth structure on Fennoscandian glacial isostatic adjustment: Implications for space-geodetic estimates of present-day crustal deformations, Geophys. Res. Lett.,33, L13502, doi:10.1029/ 2006GL026568

Wiedicke M., H.-R. Kudrass, Ch. Hubscher (1999) Oolitic beach barriers of the last Glacial sea-level lowstand at the outer Bengal shelf, *Marine Geology*, 157, 7-18

Wolstencroft, M., Z. Shen, T. E. Törnqvist, G. A. Milne, and M. Kulp (2014) Understanding subsidence in the Mississippi Delta region due to sediment, ice, and ocean loading: Insights from geophysical modeling, *J. Geophys. Res. Solid Earth*, 119, 3838-3856, doi:10.1002/2013JB010928

Woppelmann, G., M. Marcos (2016) Vertical land motion as a key to understanding sea level change and variability, *Rev. Geophysics*, 54, 64-92, doi:10.1002/2015RG000502

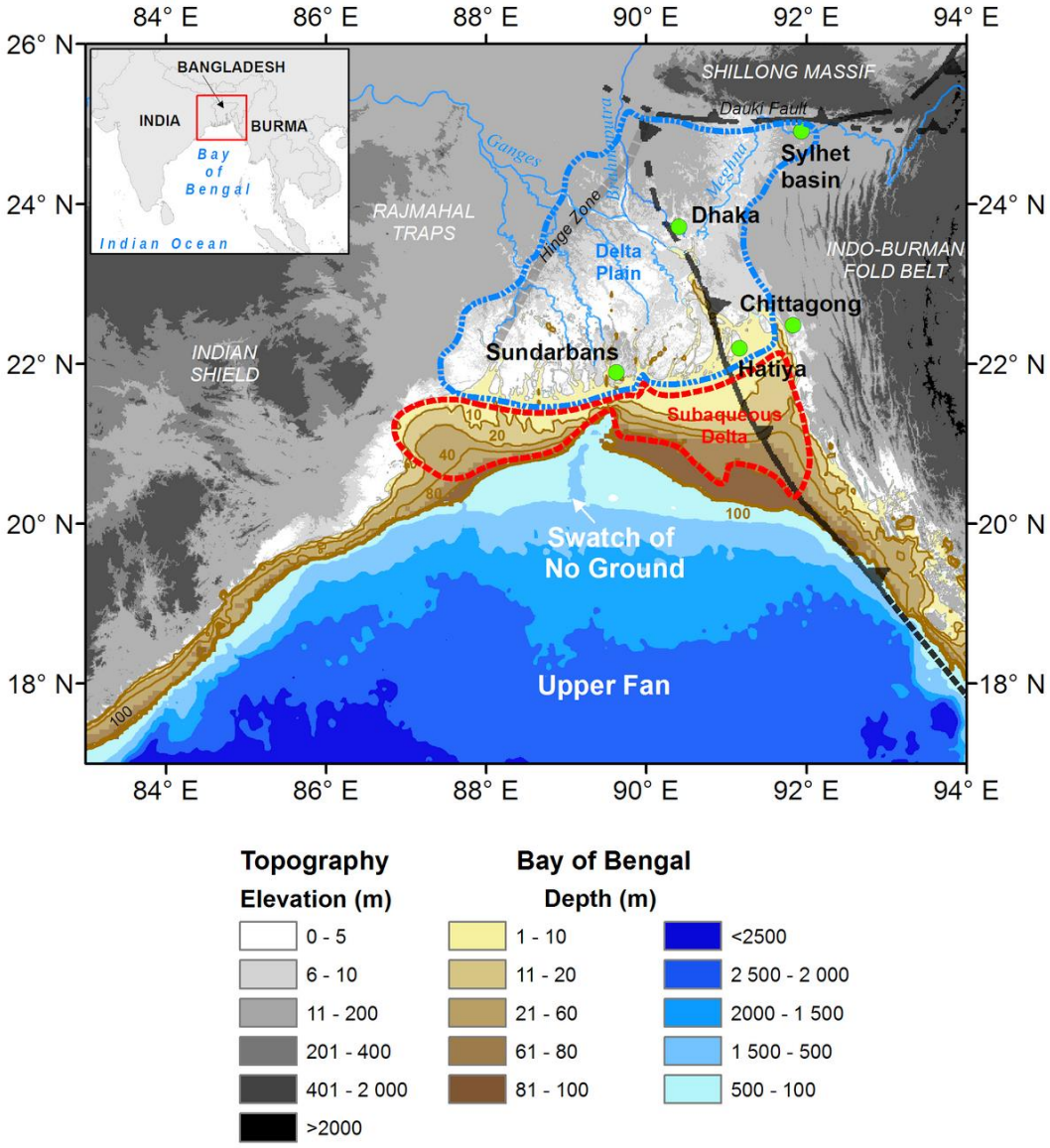

Figure 1. (a) Topographic map of the Ganges-Brahmaputra delta and the Bay of Bengal. Position of Eocene shelf edge (dashed gray line) and a possible location of thrust front of the fold belt (black barbed line) are adapted from Steckler et al. (2008). Bathymetry data are from Krien et al. (2017). Green points indicate specific sites where subsidence will be displayed as a function of time.

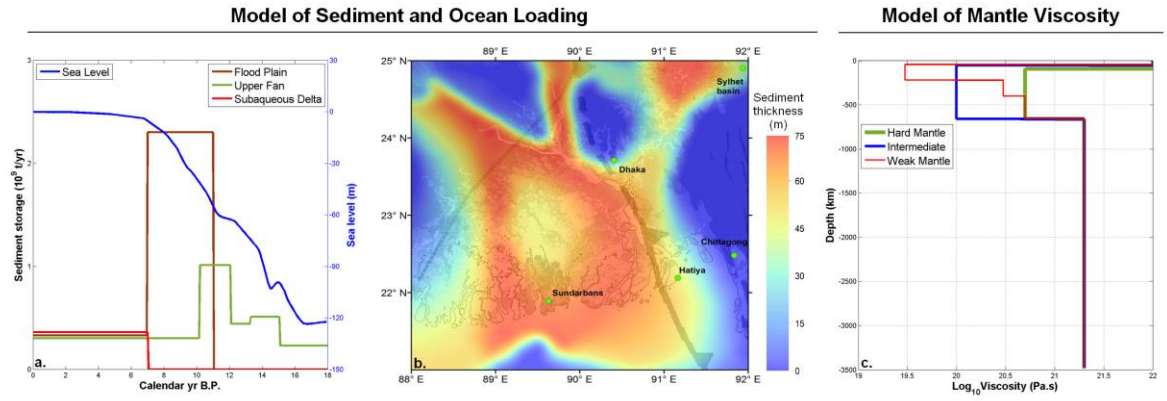

Figure 2. (a) Time history of sediment storage (Gt/yr) on the GBD flood plain (brown), subaqueous delta (red) and the upper fan (green); blue line is the eustatic sea level curve from Lambeck et al. [2014]; (b) Thickness (m) of Holocene sediments in the GBD adapted from Goodbred and Kuehl [2000] (c) Viscosity profiles representing: hard mantle (green), intermediate viscosity (blue) and weak mantle structure (red)

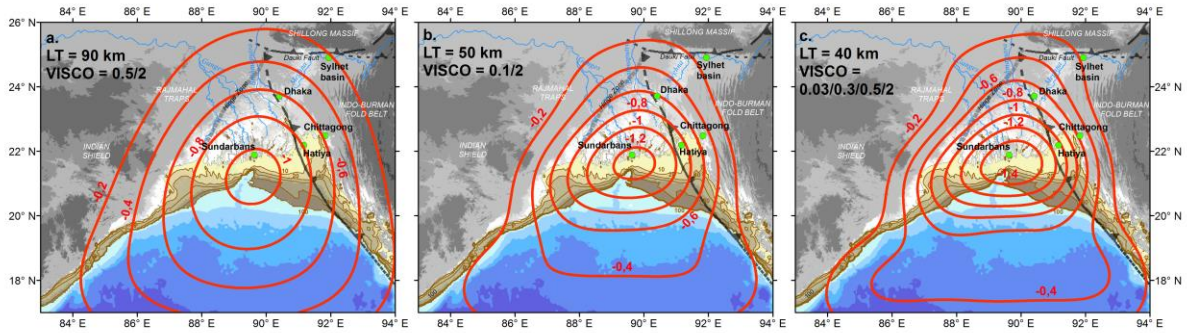

Figure 3. Predicted present-day subsidence rates (mm/yr) with rheological structures shown in Fig.2c: (a) with thick lithosphere and hard mantle, (b) intermediate structure, (c) thin lithosphere and weak mantle viscosity. Abbreviations correspond to lithospheric thickness (LT) and viscosity (VISCO) of the underlying mantle: numbers are multiplies of 10^{21} Pa s, doublets correspond to viscosity of upper and lower mantle respectively, quadruplet (c) to viscosity of asthenosphere (between LT and the 220 km depth) , shallow upper mantle (220 - 400 km), deeper upper mantle (400-670 km) and lower mantle, respectively.

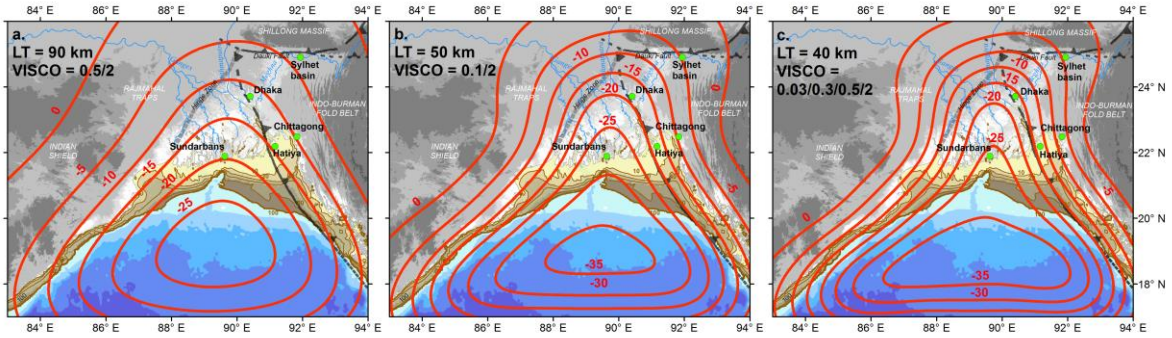

Figure 4. Net subsidence (m) since 18 000 B.P. predicted with different rheological structures: (a) thick lithosphere and hard mantle, (b) intermediate structure, (c) thin lithosphere and weak mantle viscosity. Abbreviations are the same as in Fig.3.

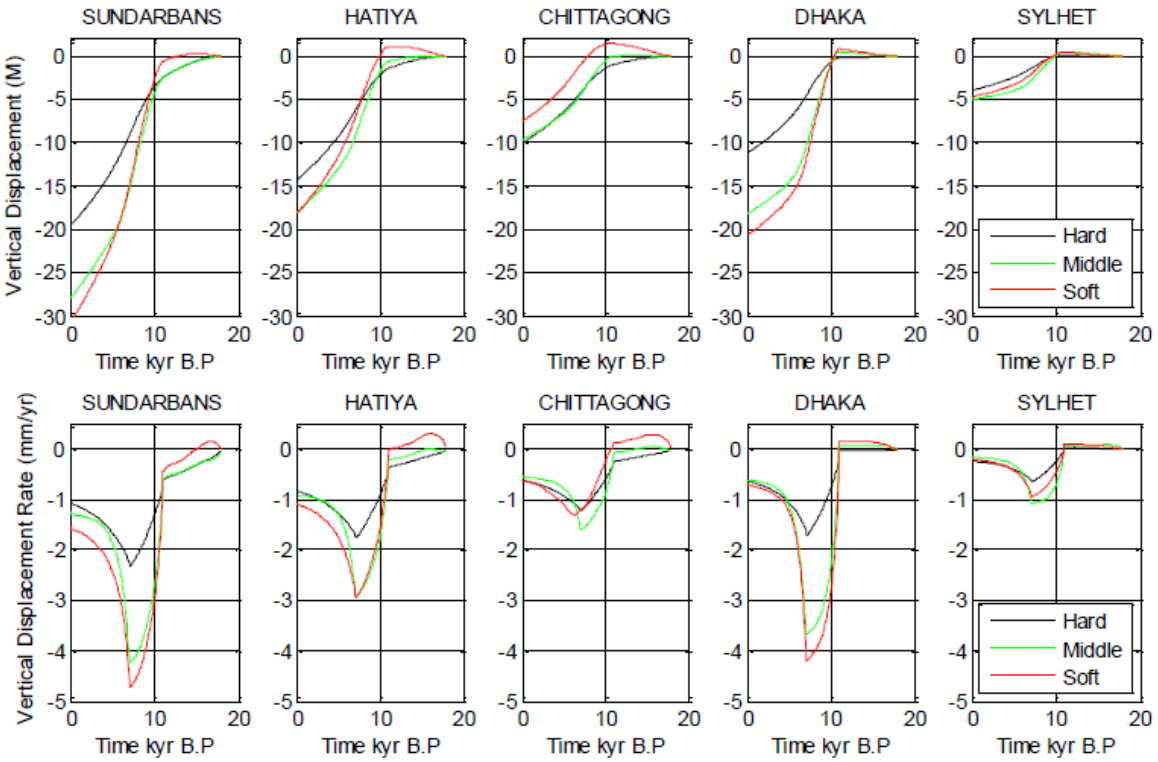

Figure 5. Vertical displacements (subsidence if <0) and displacement rates (mm/yr) computed at the specific sites marked in Fig.1: blue line – with thick lithosphere and hard mantle, green – intermediate structure, red – with thin lithosphere and weak mantle